PD-L1 is a novel direct target of HIF-1α, and its blockade under hypoxia enhanced MDSC-mediated T cell activation

Muhammad Zaeem Noman,[1] Giacomo Desantis,[2] Bassam Janji,[3] Meriem Hasmim,[1] Saoussen Karray,[1] Philippe Dessen,[4] Vincenzo Bronte,[5] and Salem Chouaib[1]

[1]Unité Institut National de la Santé et de la Recherche Médicale U753, Institut de Cancérologie Gustave Roussy, 94805 Villejuif, France
[2]Istituto Oncologico Veneto, Istituti di Ricovero e Cura a Carattere Scientifico (IRCCS), 35128 Padua, Italy
[3]Laboratory of Experimental Hemato-Oncology, Department of Oncology. Public Research Center for Health (CRP-Santé), L-1526 Luxembourg City, Luxembourg
[4]Functional Genomic Unit, Gustave Roussy Cancer Institute, 94805 Villejuif, France
[5]Department of Pathology and Diagnostics, Verona University, 37134 Verona, Italy

Tumor-infiltrating myeloid cells such as myeloid-derived suppressor cells (MDSCs) and tumor-associated macrophages (TAMs) form an important component of the hypoxic tumor microenvironment. Here, we investigated the influence of hypoxia on immune checkpoint receptors (programmed death [PD]-1 and CTLA-4) and their respective ligands (PD-1 ligand 1 [PD-L1], PD-L2, CD80, and CD86) on MDSCs. We demonstrate that MDSCs at the tumor site show a differential expression of PD-L1 as compared with MDSCs from peripheral lymphoid organ (spleen). Hypoxia caused a rapid, dramatic, and selective up-regulation of PD-L1 on splenic MDSCs in tumor-bearing mice. This was not limited to MDSCs, as hypoxia also significantly increased the expression of PD-L1 on macrophages, dendritic cells, and tumor cells. Furthermore, PD-L1 up-regulation under hypoxia was dependent on hypoxia-inducible factor-1α (HIF-1α) but not HIF-2α. Chromatin immunoprecipitation and luciferase reporter assay revealed direct binding of HIF-1α to a transcriptionally active hypoxia-response element (HRE) in the PD-L1 proximal promoter. Blockade of PD-L1 under hypoxia enhanced MDSC-mediated T cell activation and was accompanied by the down-regulation of MDSCs IL-6 and IL-10. Finally, neutralizing antibodies against IL-10 under hypoxia significantly abrogated the suppressive activity of MDSCs. Simultaneous blockade of PD-L1 along with inhibition of HIF-1α may thus represent a novel approach for cancer immunotherapy.

CORRESPONDENCE
Salem Chouaib:
chouaib@igr.fr

Abbreviations used: ChIP, chromatin immunoprecipitation; CTLA-4, cytotoxic T lymphocyte antigen 4; HIF, hypoxia-inducible factor; HRE, hypoxia response element; IMDSC, myeloid derived suppressor cell; PD, programmed death; PD-L1, PD-1 ligand 1; TAM, tumor-associated macrophage; T reg cell, regulatory T cell.

Hypoxia is a common feature of solid tumors (Semenza, 2011). Hypoxic zones in tumors attract immunosuppressive cells such as myeloid-derived suppressor cells (MDSCs; Corzo et al., 2010), tumor-associated macrophages (TAMs; Doedens et al., 2010; Imtiyaz et al., 2010), and regulatory T cells (T reg cells; Clambey et al., 2012). MDSCs are a heterogeneous group of relatively immature myeloid cells and several studies have described mechanisms of MDSC-mediated immune suppression (Gabrilovich et al., 2012). A large body of preclinical and clinical data indicates that antibody blockade of immune checkpoints can significantly enhance antitumor immunity (Pardoll, 2012; West et al., 2013). Recently, antibody-mediated blockade of pre-programmed death 1 (PD-1; Topalian et al., 2012) and its ligand, PD-L1 (Brahmer et al., 2012), was shown to result in durable tumor regression and prolonged stabilization of disease in patients with advanced cancers. PD-1, a cell surface glycoprotein with a structure similar to cytotoxic T lymphocyte antigen 4 (CTLA-4), belongs to the B7 family of co-stimulatory/co-inhibitory molecules and plays a key part in immune regulation (Greenwald et al., 2005). PD-1 has two known ligands, PD-L1 (B7-H1) and PD-L2 (B7-DC).

Although hypoxia has been shown to regulate the function and differentiation of MDSCs

The Rockefeller University Press $30.00
J. Exp. Med. 2014 Vol. 211 No. 5 781–790
www.jem.org/cgi/doi/10.1084/jem.20131916

The Journal of Experimental Medicine

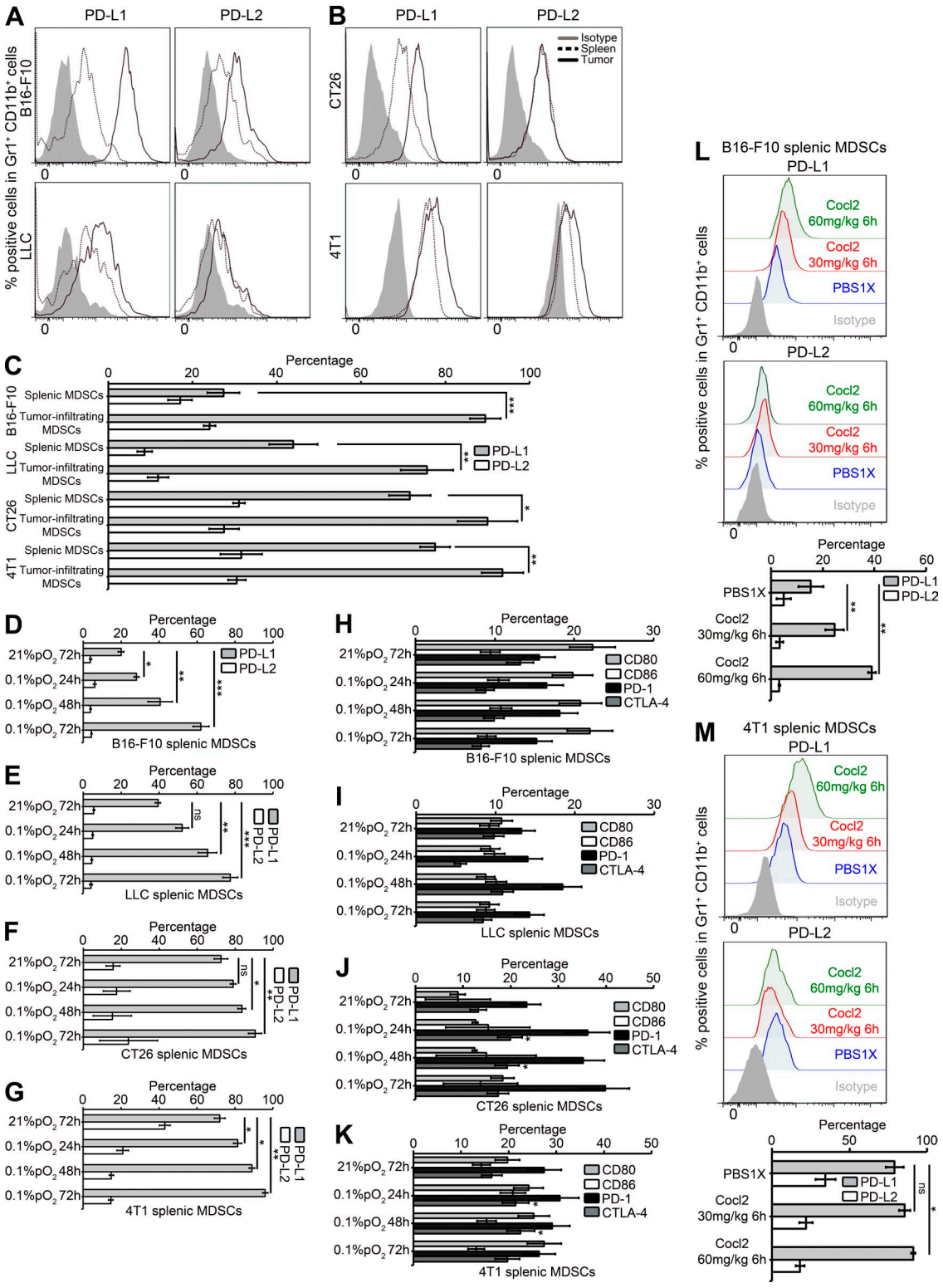

Figure 1. Tumor-infiltrating MDSCs differentially express PD-L1 as compared with splenic MDSCs, and hypoxia selectively up-regulates PD-L1 on splenic MDSCs in tumor-bearing mice. Surface expression level of PD-L1 and PD-L2 on Gr1$^+$ CD11b$^+$ cells (MDSCs) from (B16-F10 and LLC; A; CT26 and 4T1; B) in spleens (black dotted line histogram) and tumor (black line histogram) as compared with isotype control (gray-shaded histogram) was analyzed by flow cytometry. (C) Statistically significant differences (indicated by asterisks) between tumor-infiltrating MDSCs and splenic MDSCs are shown (*, $P < 0.05$; **, $P < 0.005$; ***, $P < 0.0005$). Each tumor model included $n = 5$ mice. Three experiments with the same results were performed. Error bars indicate SD. (D–G) MDSCs were isolated from spleens of B16 (D), LLC (E), CT26 (F), and 4T1 (G) tumor-bearing mice and

(Corzo et al., 2010), several major questions remain unresolved. The influence of hypoxia on the regulation of immune checkpoint receptors (PD-1 and CTLA-4) and their respective ligands (PD-L1, PD-L2, CD80, and CD86) on MDSCs remains largely obscure. Furthermore, the potential contribution of these immune checkpoint receptors and their respective ligands on MDSC function under hypoxia is still unknown.

In the present study, we showed that hypoxia via hypoxia-inducible factor-1α (HIF-1α) selectively up-regulated PD-L1 on MDSCs, but not other B7 family members, by binding directly to the HRE in the PD-L1 proximal promoter. Blockade of PD-L1 under hypoxia abrogated MDSC-mediated T cell suppression by modulating MDSCs cytokine production.

RESULTS AND DISCUSSION

Differential expression of PD-L1 on tumor-infiltrating MDSCs versus splenic MDSCs and selective up-regulation of PD-L1 in splenic MDSCs under hypoxic stress

We first compared the level of expression of PD-L1 and PD-L2 between splenic MDSCs and tumor-infiltrating MDSCs from tumor-bearing mice. We found that the percentage of PD-L1$^+$ cells was significantly higher on tumor-infiltrating MDSCs as compared with splenic MDSC in B16-F10, LLC (Fig. 1 A), CT26, and 4T1 (Fig. 1 B) tumor models. No significant difference was found in the percentage of PD-L2$^+$ cells in splenic MDSCs as compared with tumor-infiltrating MDSCs in four tumor models tested (Fig. 1 C). We did not observe any significant difference in the expression levels of other members of the B7 family such as CD80, CD86, PD-1, and CTLA-4 on MDSCs from spleen and tumor (unpublished data). Youn et al. (2008) previously observed no significant differences in the percentage of PD-L1$^+$ or CD80$^+$ cells within the splenic MDSCs from tumor-bearing mice and immature myeloid cells from naive tumor-free mice. However, by comparing the expression of immune checkpoint inhibitors between splenic and tumor-infiltrating MDSCs, we showed that there is a differential expression of PD-L1 on tumor-infiltrating MDSCs.

These data indicate that the tumor microenvironment plays a role in the regulation of PD-L1 surface expression on MDSCs. As hypoxia is one of the major components of tumor microenvironment, we tested the effect of hypoxia on the expression of immune checkpoint receptors (PD-1 and CTLA-4) and their respective ligands (PD-L1, PD-L2, CD80, and CD86) on MDSCs. Hypoxia dramatically and significantly increased the percentage of PD-L1$^+$ MDSCs isolated from spleen in B16-F10 (Fig. 1 D) and LLC (Fig. 1 E) tumor-bearing mice. Similarly, other models (CT26 and 4T1) showed a variable but significant increase in PD-L1 expression on splenic MDSCs under hypoxia (Fig. 1, F and G). However, no difference in the level of expression was observed for PD-L2 (Fig. 1, D–G), CD80, CD86, PD-1, or CTLA-4 (Fig. 1, H–K) in splenic MDSCs cultured under hypoxia in four tumor models tested.

To assess whether splenic MDSCs in tumor-bearing mice specifically up-regulated PD-L1 when mice were exposed to hypoxic conditions, we designed and performed hypoxic conditioning of live tumor-bearing mice using cobalt chloride ($CoCl_2$; Kapitsinou et al., 2010). As shown in Fig. 1 (L and M), PD-L1 expression was significantly increased in splenic MDSCs in both B16-F10 (L) and 4T1 (M) tumor-bearing mice treated with either 30 or 60 mg/kg $CoCl_2$ as compared with PBS1X. These data clearly indicate that splenic MDSCs in tumor-bearing mice significantly up-regulate PD-L1 expression when mice are exposed to hypoxia.

We also used a panel of different mouse and human tumor cell lines with different levels of PD-L1 under normoxia. Very interestingly, as shown in Fig. 2 (A–H), hypoxia significantly increased the expression of PD-L1 on B16-F10 (Fig. 2 A) and LLC cells (Fig. 2 B), as well as on T1 (Fig. 2 E) and M4T (Fig. 2 F) cells. No effect of hypoxia on PD-L2 expression was observed on all tumor cell lines tested. Moreover, we also observed a slight but significant increase in PD-L1 expression on macrophages (F4/80$^+$; Fig. 2 I) and DCs (CD11c$^+$; Fig. 2 J) isolated from C57BL/6 naive mice splenocytes cultured under hypoxia. Thus, hypoxia recapitulated the effect of the tumor microenvironment with regard to the expression of PD-L1 on MDSCs, macrophages, DCs, and tumor cells.

As shown previously by Corzo et al. (2010), we found that exposure of splenic MDSCs to hypoxia resulted in their differentiation into macrophages and DCs. Hypoxic stress resulted in a slightly more pronounced up-regulation of PD-L1 on MDSC as compared with macrophages and a lower up-regulation of PD-L1 on CD11c$^+$ cells (unpublished data). Future experiments will attempt to dissect the potential role of increased hypoxic PD-L1 on undifferentiated MDSCs (Gr1$^+$ CD11b$^+$) and differentiated MDSCs (macrophages and DCs) in mediating the immune suppression within the hypoxic tumor microenvironment.

PD-L1 is expressed on B cells, T cells, macrophages, MDSCs, and DCs and is up-regulated upon their activation (Okazaki

cultured at indicated times under normoxic and hypoxic (0.1% pO_2) conditions. Shown is the percentage of PD-L1$^+$ or PD-L2$^+$ cells among Gr1$^+$ CD11b$^+$ cells obtained from different tumor models. (H–K) Shown is the percentage of CD80$^+$, CD86$^+$, PD-1$^+$, and CTLA-4$^+$ cells among Gr1$^+$ CD11b$^+$ cells obtained from B16-F10 (H), LLC (I), CT26 (J), and 4T1 (K) tumor-bearing mice. Statistically significant differences (indicated by asterisks) between splenic MDSCs cultured under normoxia or hypoxia are shown (*, $P < 0.05$; **, $P < 0.005$; ***, $P < 0.0005$). Each tumor model included $n = 3$ mice. Three separate experiments with the same results were performed. Error bars indicate SD. (L and M) B16-F10 tumor-bearing C57BL/6 mice or 4T1 tumor-bearing BALB/c mice were injected i.p. with either PBS1X, 30 or 60 mg/kg of cobalt chloride ($CoCl_2$). Surface expression level of PD-L1 and PD-L2 on Gr1$^+$ CD11b$^+$ cells (MDSCs) from B16-F10 (L) and 4T1 (M) total splenocytes was analyzed by flow cytometry. Each tumor model included $n = 3$ mice. Statistically significant differences (indicated by asterisks) between mice treated with PBS1X or CoCl2 are shown (*, $P < 0.05$; **, $P < 0.005$). Data represent two independent experiments with SD.

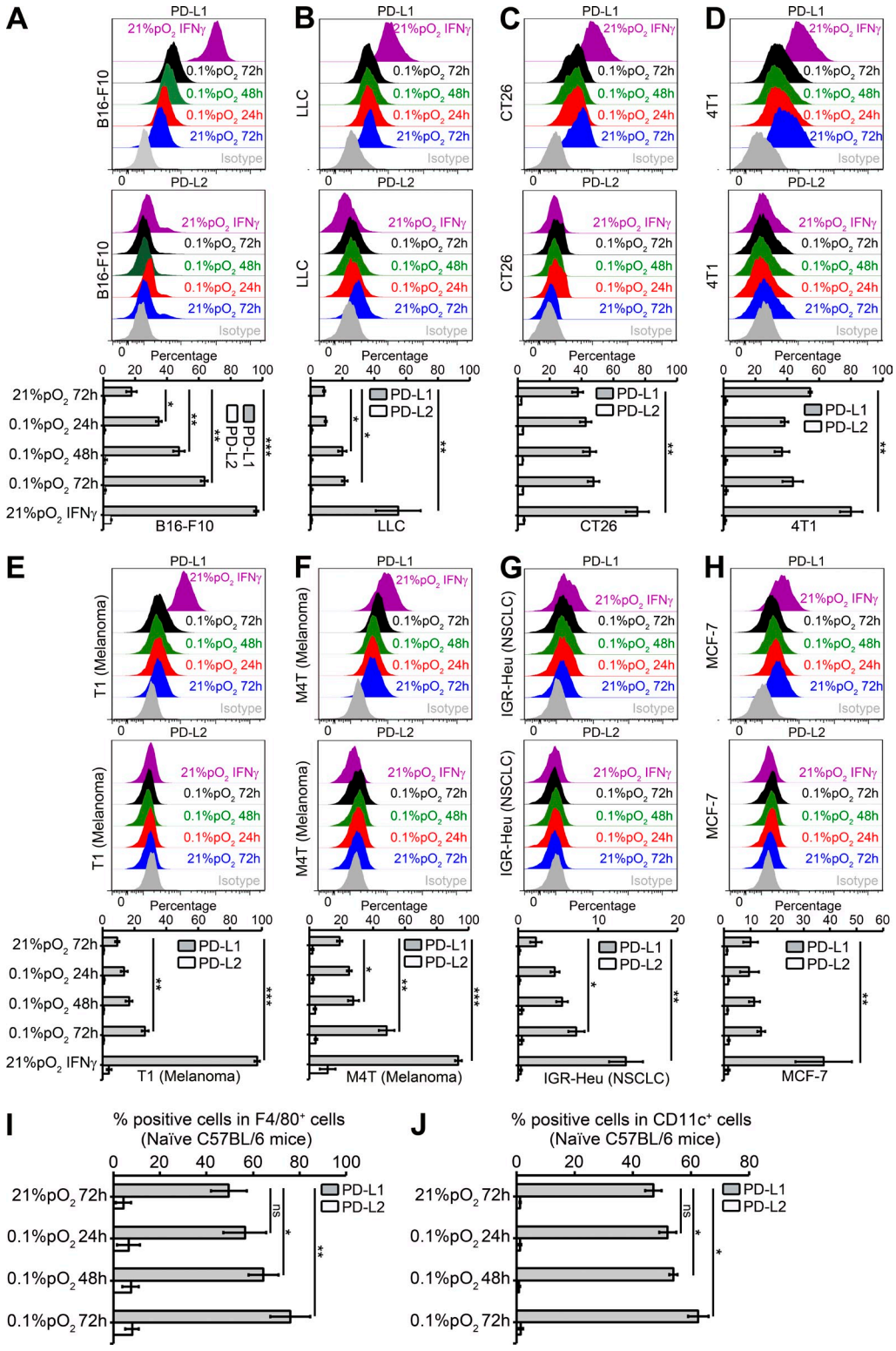

Figure 2. Hypoxia up-regulates PD-L1 on mouse and human tumor cell lines and on macrophages and DCs from naive C57BL/6 mice. (A–H) Mouse and human tumor cell lines were cultured under normoxia and hypoxia (0.1% pO_2) at indicated times. Recombinant mouse or human IFN-γ–treated (10 ng/ml) cells were used as positive control for PD-L1 induction under normoxia for 24 h. Shown is the surface expression of PD-L1 and PD-L2 on B16-F10 (A), LLC (B), CT26 (C), 4T1 (D), T1 (E), M4T (F), IGR-Heu (G), and MCF-7 (H) tumor cells. Statistically significant differences (indicated by asterisks) between tumor cells cultured under normoxia or hypoxia are shown (*, $P < 0.05$; **, $P < 0.005$; ***, $P < 0.0005$). Three separate experiments with the same results were performed. Error bars indicate SD. (I and J) C57BL/6 naive mice spleens were used for preparing single-cell suspensions by mechanical

and Honjo, 2007). PD-L1 expression on MDSCs was shown to be significantly augmented during late stages of tumor growth in *ret* melanomas (Fujimura et al., 2012). There is extensive evidence that the tumor microenvironment factor IFN-γ induced/up-regulated the expression of PD-L1 on 4T1 mammary tumors (duPre' et al., 2008), A549 lung cancer cells (Lee et al., 2006), and melanoma cells (Haile et al., 2011). Similarly, in ovarian carcinoma, microenvironmental factors like IL-10 and VEGF can modulate PD-L1 expression on monocyte-derived myeloid DCs (MDCs; Curiel et al., 2003). Our results clearly indicate that in addition to IL-10, VEGF, and IFN-γ, hypoxia is yet another novel critical modulator of PD-L1 expression on MDSCs, macrophages, DCs, and tumor cells in the tumor microenvironment. It would be of major interest to study the potential contribution of increased hypoxic PD-L1 on MDSCs, macrophages, DCs, and tumor cells in regulating the immune suppression within the hypoxic tumor microenvironment.

HIF-1α regulates the expression of PD-L1 by binding directly to the HRE in the PD-L1 proximal promoter

We further investigated whether hypoxia can regulate PD-L1 expression at both the mRNA and protein level in MDSCs. For this purpose, we took advantage of an already established MDSC cell line, MSC-1 (Apolloni et al., 2000), as it is difficult to maintain ex vivo MDSC in culture because of their rapid and spontaneous death. We first validated that hypoxia significantly increased the cell surface expression of PD-L1 but not of PD-L2, CD80, CD86, PD-1, or CTLA-4 on MSC-1 cells (Fig. 3, A and B; and not depicted). Western blot analysis further revealed that along with induction of HIF-1α and HIF-2α, PD-L1 was substantially up-regulated in MSC-1 cells under hypoxia (Fig. 3 C). Furthermore, hypoxia significantly increased the mRNA expression levels of PD-L1 and CTLA-4 but not of PD-L2 and PD-1 in MSC-1 cells (Fig. 3 D). These results were further confirmed in $Gr1^+$ MDSCs isolated from spleens in B16-F10 and 4T1 tumor-bearing mice. Fig. 3 (E and F) clearly shows that $Gr1^+$ MDSCs cultured under hypoxia significantly increased PD-L1 mRNA expression level in both models.

To dissect the roles of the HIFs (HIF-1α and HIF-2α) in PD-L1 up-regulation under hypoxia, the MSC-1 cell line was transfected with siRNA targeting HIF-1α, HIF-2α, or scrambled control (Fig. 3 G). siRNA-mediated knockdown of HIF-1α but not HIF-2α under hypoxia significantly decreased PD-L1 mRNA (Fig. 3 H) and PD-L1 protein (Fig. 3, I and J) levels in MSC-1 cells. Moreover, no effect of HIFs (HIF-1α or HIF-2α) on CD80, CD86, PD-L2, PD-1, and CTLA-4 mRNA (Fig. 3 H) or protein levels (Fig. 3 K) was observed.

To investigate whether PD-L1 is a direct HIF-1α target gene, we searched for potential HIF-1α–binding sites in the proximal promoter of mouse PD-L1 gene using fuzznuc (EMBOSS explorer) software. As shown in Fig. 3 M, we found four putative hypoxia response elements (HREs) containing the consensus sequence (A/G) CGTG within the mouse PD-L1 gene.

Using chromatin immunoprecipitation (ChIP) assay, we demonstrated hypoxia-inducible binding of HIF-1α at two different HRE sites in hypoxic MSC-1 cells (Fig. 3 L). ChIP complexes in hypoxic MSC-1 cells showed a significant binding of HIF-1α at HRE-4 and at HRE-1 (>20 fold for HRE-4), comparable to their binding to an established HRE in VEGF, LDHA, and Glut1 genes.

To determine whether this HIF-1α site (HRE-4) was a transcriptionally active HRE, MSC-1 cells were co-transfected with pGL4-hRluc/SV40 vector and pGL3 EV, pGL3 HRE-4, or pGL3 HRE-4 MUT vectors (Fig. 3 M) and grown under normoxia or hypoxia. After 48 h, firefly and renilla luciferase activities were measured. As shown in Fig. 3 N, hypoxia significantly increased the luciferase activity of HRE-4 reporter by more than threefold as compared with normoxia. More interestingly, the luciferase activity of HRE-4 MUT was significantly decreased (>50%) as compared with HRE-4 under hypoxia (Fig. 3 N). The results presented in Figs. 3 (H–N) demonstrate that PD-L1 is a direct HIF-1α target gene in MSC-1 cells.

Thus, we provide evidence here that HIF-1α is a major regulator of PD-L1 mRNA and protein expression, and that HIF-1α regulates the expression of PD-L1 by binding directly to the HRE-4 in the PD-L1 proximal promoter.

Blocking PD-L1 decreases MDSC-mediated T cell suppression under hypoxia by down-regulating MDSC IL-6 and IL-10

To directly test the functional consequences of hypoxia-induced up-regulation of PD-L1 in MDSC-mediated T cell suppression, the expression of PD-L1 was blocked on ex vivo MDSCs by using anti–PD-L1 monoclonal antibody. Hypoxia increased the ability of MDSCs to suppress both specific and nonspecific stimuli-mediated T cell proliferation (Fig. 4, A and B). Interestingly, blockade of PD-L1 under hypoxia significantly abrogated the suppressive activity of MDSCs in response to both nonspecific stimuli (anti-CD3/CD28 antibody; Fig. 4 A) and specific stimuli ($TRP\text{-}2_{(180–88)}$ peptide; Fig. 4 B). Under hypoxia, MDSCs acquired the ability to inhibit T cell function (Fig. 4, C and D) by decreasing the percentage of IFN-γ^+ $CD8^+$ and $CD4^+$ T cells; whereas the percentage of IFN-γ^+ $CD8^+$ (Fig. 4 C) and IFN-γ^+ $CD4^+$ T cells (Fig. 4 D) significantly increased after PD-L1 blockade

dissociation, followed by removal of red blood cells with ammonium chloride lysis buffer (ACK). Macrophages and DCs were further isolated by cell sorting on FACS MoFlo or FACSAria (BD) after incubating with F4/80+ PE or CD11c+ APC-conjugated antibodies, respectively. The sorted F4/80+ PE (I) and CD11c+ APC (J) cells were incubated under normoxia or hypoxia (0.1% pO_2) for 24, 48, and 72 h, and PD-L1 and PD-L2 expression was evaluated by flow cytometry. Statistically significant differences (indicated by asterisks) between macrophages and DCs incubated under normoxia or hypoxia are shown (*, $P < 0.05$; **, $P < 0.005$). The experiment was performed with $n = 3$ mice and repeated twice with the same results. Error bars indicate SD.

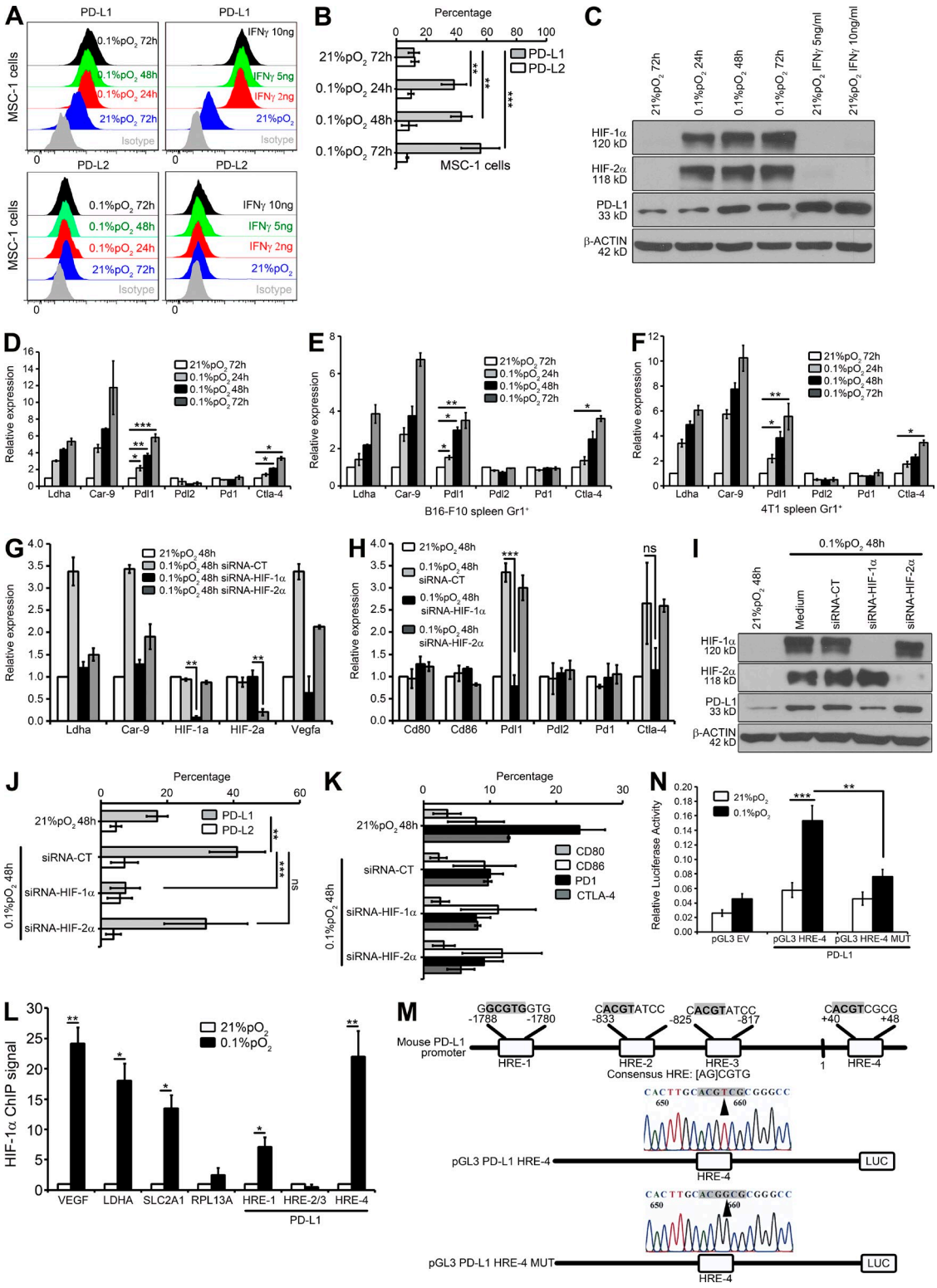

Figure 3. HIF-1α binds directly to the HRE in the PD-L1 proximal promoter and up-regulates its expression under hypoxia. (A–F) Surface expression levels of PD-L1 and PD-L2 (A and B) on MSC-1 cells cultured under normoxia and hypoxia (0.1% pO_2) at indicated times as compared with isotype control (gray-shaded histogram). IFN-γ was used as a positive control for PD-L1 up-regulation. Statistically significant differences (indicated by asterisks) between MSC-1 cells cultured under normoxia or hypoxia are shown (**, $P < 0.005$; ***, $P < 0.0005$). Three separate experiments with the same results were performed. Error bars indicate SD. (C) Western blot was performed to show HIF-1α, HIF-2α, and PD-L1 protein levels. β-Actin was used as a control. Three separate experiments with the same results were performed. (D–F) SYBR Green RT-qPCR was used to monitor Ldha, Car-9, Pdl1, Pdl2, Pd1,

under hypoxic conditions. Thus, the immune suppressive function of MDSCs enhanced under hypoxia was abrogated after blocking PD-L1, and hypoxic up-regulation of PD-L1 on MDSCs is involved in mediating the suppressive action of MDSCs, at least in part, as we were not able to completely restore T cell proliferation and function after PD-L1 blockade on MDSCs under hypoxia.

It is important to underline that our results are in complete agreement with previous findings by Youn et al. (2008), indicating that normoxic blockade of PD-L1 did not eliminate suppressive activity of MDSCs. In line with our data, blockade of tumor microenvironment induced PD-L1 on MDCs has been shown to enhance MDC-mediated T cell activation (Curiel et al., 2003). Similarly, in *ret* oncogene-driven melanomas, decreased IL-10 production from T reg cells modulated PD-L1 expression in MDSCs and decreased their immunosuppressive phenotype (Fujimura et al., 2012).

To determine the underlying mechanism involved in the attenuation of immune suppressive activity of MDSCs under hypoxia after PD-L1 blockade, we examined the effects of treatment with anti–PD-L1 monoclonal antibody on MDSC function in terms of their arginase activity and NO production. As shown previously by Corzo et al. (2010), we observed higher levels of Arg-1 gene expression (Fig. 4 E) and arginase activity (Fig. 4 F), as well as Nos-2 gene expression (Fig. 4 E) and NO production (Fig. 4 G) in hypoxic MDSCs. However, we observed no effect on either on Arg-1 gene (Fig. 4 E) and arginase activity (Fig. 4 F) or on Nos-2 expression (Fig. 4 E) and NO production (Fig. 4 G) in hypoxic MDSCs after PD-L1 blockade, indicating that PD-L1 does not control these pathways.

We next evaluated the effect of hypoxia on the production and secretion of different cytokines (IL-6, IL-10, and TGF-β1) by MDSCs. As shown in Fig. 4 H, MDSCs cultured under hypoxia expressed substantially higher levels of Il-6, Il-10, and Tgf-b1, but not Il-12. Antibody blocking PD-L1 had no effect on the expression of these genes under normoxia. In contrast, hypoxia blockade of PD-L1 in MDSCs significantly decreased Il-6 and Il-10, but not Tgf-b1 expression levels (Fig. 4 H). Furthermore, using FACS analysis, intracellular cytokine staining was performed for IL-6, IL-10, IL-12p70, and TGF-β1. Hypoxia resulted in a significant increase in intracellular IL-6, IL-10, and TGF-β1 in MDSCs (Fig. 4, I and J). Strikingly, PD-L1 blockade significantly decreased the IL-6 and IL-10, but not TGF-β1, production in MDSCs under hypoxia (Fig. 4 J). ELISA was used to confirm the cytokine production under hypoxia. Hypoxia significantly increased secreted levels of IL-6, IL-10, and TGF-β1 from MDSCs, but this hypoxia up-regulated secretion of IL-6 and IL-10 in MDSCs was significantly attenuated after blocking with PD-L1–specific antibody (Fig. 4 K). Finally, neutralizing antibodies against IL-10 but not IL-6 under hypoxia significantly abrogated the suppressive activity of MDSCs in response to nonspecific stimuli (anti-CD3/CD28 antibody; Fig. 4 L) and specific stimuli ($TRP\text{-}2_{[180–88]}$ peptide; Fig. 4 M). Similarly, MDSC's increased ability to inhibit T cell function under hypoxia significantly decreased only with IL-10–neutralizing antibody, as the percentage of IFN-γ^+ $CD8^+$ T cells (Fig. 4 N) and IFN-γ^+ $CD4^+$ (Fig. 4 O) T cells significantly increased with IL-10–blocking antibody. Thus, we can conclude that blockade of PD-L1 or neutralizing IL-10 under hypoxia abrogated MDSC-mediated T cell suppression. In agreement with our results, in a murine model of ovarian cancer, MDSCs but not T reg cells were the predominant source of IL-10. Blockade of IL-10 signaling resulted in the abrogation of MDSC-mediated immunosuppression, improved T cell function, and decreased tumor progression (Hart et al., 2011). Future experiments will focus on the elucidation of the mechanism associated with anti–PD-L1 blockade-induced decrease in IL-6 and IL-10 production in hypoxic MDSC cells.

Hypoxia selectively up-regulated only PD-L1 on MDSCs via HIF-1α by binding directly to the hypoxia-response element (HRE) in the PD-L1 proximal promoter. Blockade of PD-L1 under hypoxia abrogated MDSC-mediated T cell suppression in part by modulating cytokine production, particularly of IL-6 and IL-10 in hypoxic MDSCs. Our results establish

and Ctla-4 expressions levels at indicated conditions in MSC-1 (D), B16-F10 spleen $Gr1^+$ (E), and 4T1 spleen $Gr1^+$ (F) cells. Expression level of 18S was used as endogenous control. Statistically significant differences (indicated by asterisks) between cells (MSC-1 or spleen $Gr1^+$) cultured under normoxia or hypoxia are shown (*, $P < 0.05$; **, $P < 0.005$; ***, $P < 0.0005$). Three separate experiments (in triplicates) with the same results were performed. Error bars indicate SD. (G–K) MSC-1 cells were transfected with different siRNA targeting HIF-1α, HIF-2α, or scrambled control (CT) and cultured under normoxia or hypoxia for 48 h. Expression levels of Ldha, Car-9, HIF-1α, HIF-2α, and Vegfa (G) and Cd80, Cd86, Pdl1, Pdl2, Pd1, and Ctla-4 (H) were evaluated by SYBR Green RT-qPCR. (I) Western blot was performed to show HIF-1α, HIF-2α, and PD-L1 protein levels. β-Actin was used as a control. (J) Surface expression levels of PD-L1 and PD-L2 were determined by flow cytometry. (K) Surface expression levels of CD80, CD86, PD-1, and CTLA-4 were determined by flow cytometry. Statistically significant differences (indicated by asterisks) between MSC-1 cells transfected with either siRNA-CT and siRNA-HIF-1α are shown (*, $P < 0.05$; **, $P < 0.005$; ***, $P < 0.0005$). The experiment was repeated three times with the same results. Error bars indicate SD. (L) MSC-1 cells were cultured at normoxia or hypoxia (0.1% pO_2) and ChIP was performed using anti-HIF-1α antibody followed by SYBR Green RT-qPCR using Vegfa, Ldha, Slc2a1, and Pdl1 HRE sites (HRE-1, HRE-2/3, and HRE-4) and RPL13A primers. For each gene, the RT-qPCR signals were normalized to the normoxic condition. Statistically significant differences (indicated by asterisks) between normoxic and hypoxic conditions are shown (*, $P < 0.05$; **, $P < 0.005$). Two separate experiments (in triplicates) with the same results were performed. Error bars indicate SD. (M) Different HREs in mouse PD-L1 promoter (PD-L1 mRNA; NCBI reference sequence NM_021893.3) are shown. The numbering scheme is from the refseq RNA start. (N) MSC-1 cells were co-transfected with pGL4-hRluc/SV40 vector and pGL3 empty vector (pGL3 EV), pGL3 HRE-4, or pGL3 HRE-4 MUT vectors and grown under normoxia or hypoxia. After 48 h, firefly and renilla luciferase activities were measured using the Dual-Luciferase Reporter assay (Promega) and the ratio of firefly/Renilla luciferase was determined. Statistically significant differences (indicated by asterisks) between normoxic and hypoxic conditions are shown (**, $P < 0.005$; ***, $P < 0.0005$). The experiment was performed in triplicates and repeated three times with the same results. Error bars indicate SD.

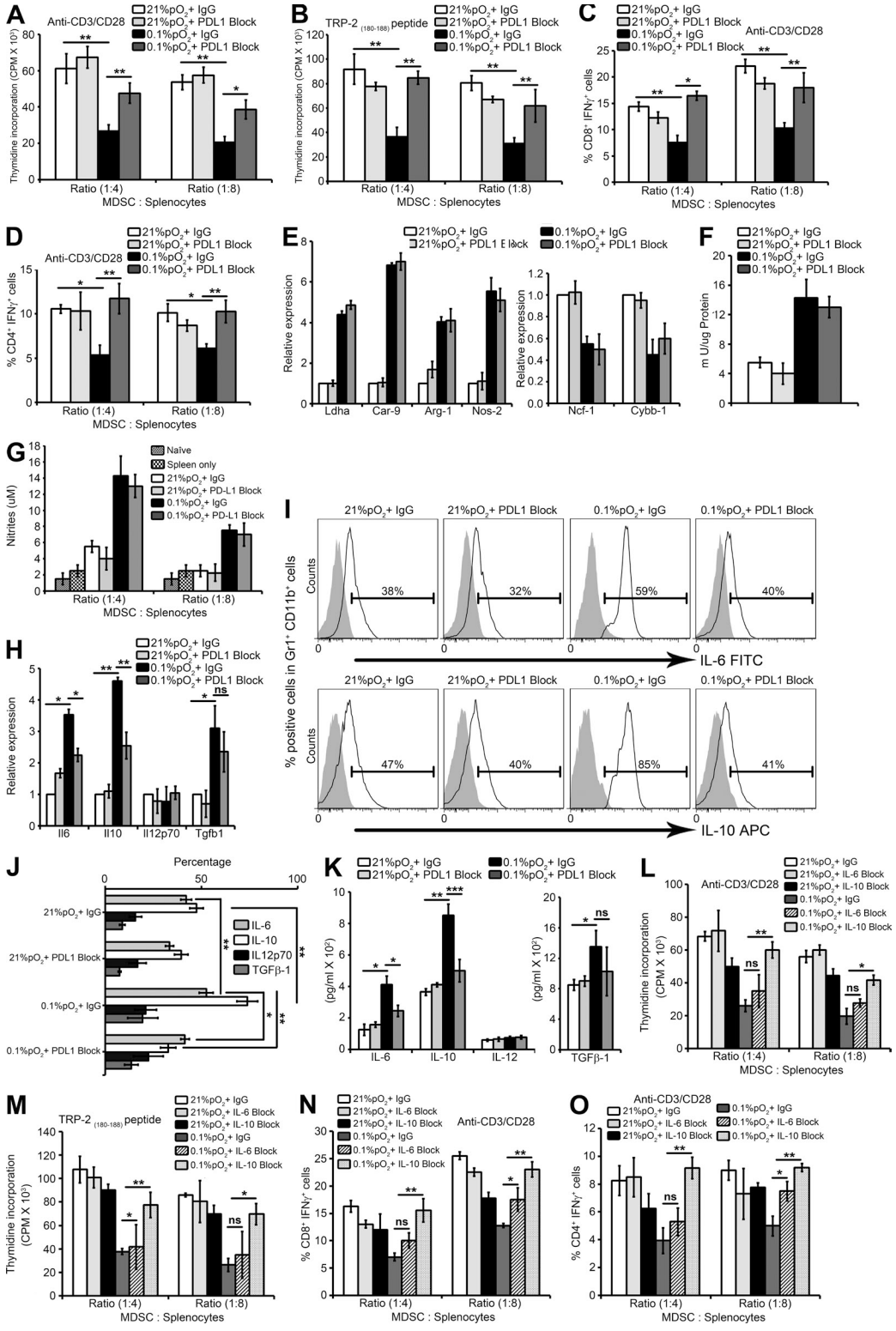

Figure 4. Blockade of PD-L1 under hypoxia down-regulates MDSC IL-6 and IL-10 and enhances T cell proliferation and function. MDSCs isolated from spleens of B16-F10 tumor-bearing mice were pretreated for 30 min on ice with 5 µg/ml control antibody (IgG) or antibody against PD-L1 (PDL1 Block) and co-cultured with splenocytes under normoxia and hypoxia for 72 h. (A and B) Effect of MDSC on proliferation of splenocytes stimulated with (A) anti-CD3/CD28 coated beads or (B) TRP-$2_{(180–88)}$ peptide under the indicated conditions. Cell proliferation was measured in triplicates by [^{3}H]thymidine incorporation and expressed as counts per minute (CPM). (C and D) MDSCs were cultured with splenocytes from B16-F10 mice stimulated with anti-CD3/CD28. Intracellular IFN-γ production was evaluated by flow cytometry by gating on (C) $CD3^+CD8^+$ IFN-γ^+ and (D) $CD3^+CD4^+$ IFN-γ^+ populations. Statistically

a new link between the immune checkpoint inhibitor PD-L1 and MDSC-mediated immune suppression under hypoxia in the tumor microenvironment.

Therefore, a combinational therapy targeting tumor hypoxia by using HIF-1α inhibitors along with PD-L1 blockade may be beneficial for boosting the immune system in cancer patients.

MATERIALS AND METHODS

Mice and tumor models. Female C57BL/6 (Charles River) and BALB/c (Harlan) mice were housed at Gustave Roussy animal facility and experiments respected EU Directive 63/2010. All experiments with mice were approved by Animal Experimentation and Ethics Committee of the Institut Gustave Roussy (CEEA IRCIV/IGR n° 26, registered at the French Ministry of Research). 7–8-week-old mice (n = 5 per group) were inoculated s.c. with the following mouse tumor cells: B16-F10 melanoma, Lewis Lung Carcinoma (LLC), CT26 colon carcinoma, and 4T1 mammary carcinoma, all obtained from American Type Culture Collection (ATCC). Different numbers of tumor cells were inoculated for different models. Tumors were used when they reached ∼1.5 cm diam. MDSC immortalized cell line MSC-1 was provided by V. Bronte (Verona University, Verona, Italy).

Reagents and antibodies. RPMI 1640, DMEM, FBS, and antibiotics were obtained from Life Technologies. Recombinant murine GM-CSF, anti–TGFB1-APC, and IL-2 were obtained from R&D Systems. The following antibodies were purchased from eBioscience: anti-Gr1 FITC, anti-Gr1 PE, anti-F4/80$^+$ PE, anti-Cd11b$^+$ PE, anti-CD11c$^+$ APC, anti–PD-L1 PE, anti–PD-L1 FITC, anti–PD-L1 APC, anti–PD-L2 PE, anti-CD80 FITC, anti-CD86 FITC, anti–PD-1 APC, anti–CTLA-4 APC, anti-CD4 FITC, anti-CD8 FITC, anti–IFN-γ PE-cy7, anti-IL6 FITC, anti-IL10 APC, anti-IL12p70 PE, and functional grade anti–PD-L1 (MIH5) neutralizing antibody. For blocking, control antibody (IgG; rat IgG2b K Isotype Control Functional Grade Purified; eBioscience), anti–mouse IL-6 Functional Grade Purified neutralizing antibody (eBioscience), or anti–mouse IL-10 Functional Grade Purified neutralizing antibody (eBioscience) were used.

Hypoxic conditioning of MDSCs and tumor-bearing mice. MDSCs were cultured in RPMI medium containing 10 ng/ml GM-CSF under hypoxia (0.1% pO_2 with 5% CO_2) in a hypoxia chamber (InVivo2 400 Hypoxia Workstation; Ruskinn). For $CoCl_2$ experiments, B16-F10 tumor-bearing C57BL/6 mice or 4T1 tumor-bearing BALB/c mice were injected i.p. with PBS1X and either 30 or 60 mg/kg of $CoCl_2$ (200 µl per mice). After 6 h, mice were sacrificed and spleens were used for preparing single-cell suspensions by mechanical dissociation followed by removal of red blood cells with ammonium chloride lysis buffer (ACK). Total splenocytes were immediately stained for MDSCs (Gr1$^+$ CD11b$^+$), macrophages (F4/80$^+$), and DCs (CD11c$^+$) along with either PD-L1-PE or PD-L2-FITC conjugated antibodies and analyzed by flow cytometry.

SYBR Green real-time (RT)-qPCR and Western blot. SYBR Green RT-qPCR and Western blot (rabbit anti–PD-L1 antibody; Abcam) were performed as described previously (Noman et al., 2012).

Flow cytometry analysis. Flow cytometry was performed using a FACS LSR-II (BD). Data were further analyzed by FACS DIVA 7.0 (BD) or Flow Jo 7.6.5 software (Tree Star).

Gene silencing by RNA interference. Predesigned siRNA against HIF-1α, HIF-2α, and scrambled control were obtained from Ambion and transfected by electroporation as described previously (Noman et al., 2009).

MDSC isolation from spleens and tumors. Single-cell suspensions were prepared from spleens by mechanical dissociation, followed by removal of red blood cells with ammonium chloride lysis buffer (ACK). MDSCs were further isolated by cell sorting on FACS MoFlo or FACSAria (BD) after incubating with APC-conjugated anti–Gr-1 antibody and FITC-conjugated anti-CD11b antibodies. Solid tumors were dissected and mechanically dissociated into small, <4-mm fragments with a scalpel, followed by digestion with mouse tumor dissociation kit (Miltenyi Biotec) for 45 min at 37°C. After single-cell suspensions were obtained, red blood cells were removed by ACK and dead cells were depleted with a dead cell removal kit (Miltenyi Biotec). Gr1$^+$ cells were further isolated by using either biotinylated or anti–Gr1-APC antibody and corresponding streptavidin or anti-APC microbeads on MACSLS columns according to the manufacturer's protocol (Miltenyi Biotec). This process yielded Gr1$^+$ cells with purity >95% as evaluated by FACS analysis.

MDSC functional assays. For evaluation of T cell proliferation, splenocytes from B16-F10 mice were plated into U-bottom 96-well plates along with MDSCs at different ratios (50,000 MDSC:200,000 splenocytes/well). Plates were stimulated with either anti-CD3/CD28 beads (Miltenyi Biotec) or TRP-2 180–88 peptide for 72 h at 37°C. Co-cultures were pulsed with thymidine (1 µCi/well; Promega) for 16–18 h before harvesting, and [^{3}H]thymidine uptake was counted using Packard's TopCount NXT liquid scintillation counter and expressed as counts per minute (CPM). For assessment of T cell functions, MDSCs co-cultured with splenocytes from B16-F10 mice were stimulated with anti-CD3/CD28 beads. After 72 h, intracellular IFN-γ production was evaluated by flow cytometry by gating on CD3$^+$CD8$^+$ IFN-γ$^+$ and CD3$^+$CD4$^+$ IFN-γ$^+$ populations.

MDSCs cytokine production (ELISA). MDSCs isolated from spleens of B16-F10 tumor-bearing mice were pretreated for 30 min on ice with 5 µg/ml control antibody (IgG) or Anti-Mouse PD-L1 (B7-H1) Functional Grade Purified antibody 5 µg/ml (clone MIH5; eBioscience; PDL1 Block) and cultured under normoxia and hypoxia for 72 h. Supernatants were collected and the secretion of IL-6, IL-10, and IL-12p70 (eBioscience) was determined by ELISA.

significant differences (indicated by asterisks) are shown (**, P < 0.005; ***, P < 0.0005). Three separate experiments (in triplicates) with the same results were performed. Error bars indicate SD. (E) SYBR-GREEN RT-qPCR was performed to evaluate the mRNA expression levels of Ldha, Car-9, Arg-1, Nos2, Ncf-1, and Cybb-1. (F) Arginase enzymatic activity measured in MDSCs under indicated conditions. (G) After 72 h of MDSC co-culture with splenocytes, supernatants were collected and assayed for nitrites. Data represents three independent experiments with SD. (H) SYBR Green RT-qPCR was performed for expression levels of IL6, IL10, Il12p70, and Tgfb1 under the indicated conditions. IL-6, IL-10, IL-12p70, and TGF-β1 cytokine production and secretion was detected by (I and J) intracellular FACS staining (isotype control is gray-shaded histogram) and (K) ELISA, respectively. Statistically significant differences (indicated by asterisks) are shown (*, P < 0.05; **, P < 0.005; ***, P < 0.0005). The experiment was performed in triplicates and repeated three times with the same results. Error bars indicate SD. (L–O) MDSCs isolated from spleens of B16-F10 tumor-bearing mice were co-cultured with splenocytes under normoxia and hypoxia for 72 h in the presence of either 10 µg/ml control antibody (IgG), anti–mouse IL-6 Functional Grade Purified neutralizing antibody (IL-6 Block) or anti–mouse IL-10 Functional Grade Purified neutralizing antibody (IL-10 Block). Effect of MDSCs on proliferation of splenocytes stimulated with (L) anti-CD3/CD28–coated beads or (M) TRP-$2_{(180–88)}$ peptide under the indicated conditions. Cell proliferation was measured as indicated above. MDSCs were cultured with splenocytes from B16-F10 mice stimulated with anti-CD3/CD28. Intracellular IFN-γ production was evaluated by flow cytometry by gating on (N) CD3$^+$CD8$^+$ IFN-γ$^+$ and (O) CD3$^+$CD4$^+$ IFN-γ$^+$ populations. Statistically significant differences (indicated by asterisks) are shown (*, P < 0.05; **, P < 0.005). Two separate experiments (in triplicates) with the same results were performed. Error bars indicate SD.

ChIP assay. ChIP was performed with lysates prepared from MSC-1 by using SimpleChIP Enzymatic Chromatin IP kit (Cell Signaling Technology). SYBR Green RT-qPCR was performed using the primers detailed in Table S1.

Arginase enzymatic activity and NO (nitric oxide) production. Arginase activity was measured in MDSC cell lysates, and for NO production, culture supernatants were mixed with Greiss reagent and nitrite concentrations were determined as described earlier (Youn et al., 2008).

Luciferase reporter assay. A 653-bp section corresponding to mouse PD-L1 promoter containing HRE4 sequence was inserted into the NheI–XhoI sites of pGL3-Basic vector (Promega). Mutation of HRE4 was performed by site-directed mutagenesis and verified by sequencing. A 56-bp mouse PD-L1 gene sequence was inserted into the Bgl II site of pGL3-Promoter (Promega). MSC-1 cells were co-transfected with 0.2 µg of pGL4-hRluc/SV40 vector (which contains renilla luciferase sequences downstream of the SV40 promoter) and 1 µg of pGL3 empty vector, pGL3 HRE-4, or pGL3 HRE-4 MUT vectors in 6-well plates with Lipofectamine 2000 (Invitrogen) in OPTIMEM (Invitrogen) medium and grown under normoxia or hypoxia. After 48 h, firefly and Renilla luciferase activities were measured using the Dual-Luciferase Reporter assay (Promega) and the ratio of firefly/Renilla luciferase was determined.

Statistics. Data were analyzed with GraphPad Prism. Student's *t* test was used for single comparisons.

Online supplemental material. Table S1 shows genomic oligonucleotide primers used for amplification of immunoprecipitated DNA samples from ChIP assays. Online supplemental material is available at http://www.jem.org/cgi/content/full/jem.20131916/DC1.

This work was supported by the Association pour la Recherche sur le Cancer (2012-2013: N° SFI20121205624), Ligue contre le Cancer, and CRP-Santé Luxembourg (grant LHCE-20131105).

The authors declare no conflicting financial interests.

Submitted: 10 September 2013
Accepted: 14 April 2014

REFERENCES

Apolloni, E., V. Bronte, A. Mazzoni, P. Serafini, A. Cabrelle, D.M. Segal, H.A. Young, and P. Zanovello. 2000. Immortalized myeloid suppressor cells trigger apoptosis in antigen-activated T lymphocytes. *J. Immunol.* 165:6723–6730.

Brahmer, J.R., S.S. Tykodi, L.Q. Chow, W.J. Hwu, S.L. Topalian, P. Hwu, C.G. Drake, L.H. Camacho, J. Kauh, K. Odunsi, et al. 2012. Safety and activity of anti-PD-L1 antibody in patients with advanced cancer. *N. Engl. J. Med.* 366:2455–2465. http://dx.doi.org/10.1056/NEJMoa1200694

Clambey, E.T., E.N. McNamee, J.A. Westrich, L.E. Glover, E.L. Campbell, P. Jedlicka, E.F. de Zoeten, J.C. Cambier, K.R. Stenmark, S.P. Colgan, and H.K. Eltzschig. 2012. Hypoxia-inducible factor-1 alpha-dependent induction of FoxP3 drives regulatory T-cell abundance and function during inflammatory hypoxia of the mucosa. *Proc. Natl. Acad. Sci. USA.* 109:E2784–E2793. http://dx.doi.org/10.1073/pnas.1202366109

Corzo, C.A., T. Condamine, L. Lu, M.J. Cotter, J.I. Youn, P. Cheng, H.I. Cho, E. Celis, D.G. Quiceno, T. Padhya, et al. 2010. HIF-1α regulates function and differentiation of myeloid-derived suppressor cells in the tumor microenvironment. *J. Exp. Med.* 207:2439–2453. http://dx.doi.org/10.1084/jem.20100587

Curiel, T.J., S. Wei, H. Dong, X. Alvarez, P. Cheng, P. Mottram, R. Krzysiek, K.L. Knutson, B. Daniel, M.C. Zimmermann, et al. 2003. Blockade of B7-H1 improves myeloid dendritic cell-mediated antitumor immunity. *Nat. Med.* 9:562–567. http://dx.doi.org/10.1038/nm863

Doedens, A.L., C. Stockmann, M.P. Rubinstein, D. Liao, N. Zhang, D.G. DeNardo, L.M. Coussens, M. Karin, A.W. Goldrath, and R.S. Johnson. 2010. Macrophage expression of hypoxia-inducible factor-1 alpha suppresses T-cell function and promotes tumor progression. *Cancer Res.* 70:7465–7475. http://dx.doi.org/10.1158/0008-5472.CAN-10-1439

duPre', S.A., D. Redelman, and K.W. Hunter Jr. 2008. Microenvironment of the murine mammary carcinoma 4T1: endogenous IFN-gamma affects tumor phenotype, growth, and metastasis. *Exp. Mol. Pathol.* 85:174–188. http://dx.doi.org/10.1016/j.yexmp.2008.05.002

Fujimura, T., S. Ring, V. Umansky, K. Mahnke, and A.H. Enk. 2012. Regulatory T cells stimulate B7-H1 expression in myeloid-derived suppressor cells in ret melanomas. *J. Invest. Dermatol.* 132:1239–1246. http://dx.doi.org/10.1038/jid.2011.416

Gabrilovich, D.I., S. Ostrand-Rosenberg, and V. Bronte. 2012. Coordinated regulation of myeloid cells by tumours. *Nat. Rev. Immunol.* 12:253–268. http://dx.doi.org/10.1038/nri3175

Greenwald, R.J., G.J. Freeman, and A.H. Sharpe. 2005. The B7 family revisited. *Annu. Rev. Immunol.* 23:515–548. http://dx.doi.org/10.1146/annurev.immunol.23.021704.115611

Haile, S.T., J.J. Bosch, N.I. Agu, A.M. Zeender, P. Somasundaram, M.K. Srivastava, S. Britting, J.B. Wolf, B.R. Ksander, and S. Ostrand-Rosenberg. 2011. Tumor cell programmed death ligand 1-mediated T cell suppression is overcome by coexpression of CD80. *J. Immunol.* 186:6822–6829. http://dx.doi.org/10.4049/jimmunol.1003682

Hart, K.M., K.T. Byrne, M.J. Molloy, E.M. Usherwood, and B. Berwin. 2011. IL-10 immunomodulation of myeloid cells regulates a murine model of ovarian cancer. *Front Immunol.* 2:29. http://dx.doi.org/10.3389/fimmu.2011.00029

Imtiyaz, H.Z., E.P. Williams, M.M. Hickey, S.A. Patel, A.C. Durham, L.J. Yuan, R. Hammond, P.A. Gimotty, B. Keith, and M.C. Simon. 2010. Hypoxia-inducible factor 2alpha regulates macrophage function in mouse models of acute and tumor inflammation. *J. Clin. Invest.* 120:2699–2714. http://dx.doi.org/10.1172/JCI39506

Kapitsinou, P.P., Q. Liu, T.L. Unger, J. Rha, O. Davidoff, B. Keith, J.A. Epstein, S.L. Moores, C.L. Erickson-Miller, and V.H. Haase. 2010. Hepatic HIF-2 regulates erythropoietic responses to hypoxia in renal anemia. *Blood.* 116:3039–3048. http://dx.doi.org/10.1182/blood-2010-02-270322

Lee, S.J., B.C. Jang, S.W. Lee, Y.I. Yang, S.I. Suh, Y.M. Park, S. Oh, J.G. Shin, S. Yao, L. Chen, and I.H. Choi. 2006. Interferon regulatory factor-1 is prerequisite to the constitutive expression and IFN-gamma-induced upregulation of B7-H1 (CD274). *FEBS Lett.* 580:755–762. http://dx.doi.org/10.1016/j.febslet.2005.12.093

Noman, M.Z., S. Buart, J. Van Pelt, C. Richon, M. Hasmim, N. Leleu, W.M. Suchorska, A. Jalil, Y. Lecluse, F. El Hage, et al. 2009. The cooperative induction of hypoxia-inducible factor-1 alpha and STAT3 during hypoxia induced an impairment of tumor susceptibility to CTL-mediated cell lysis. *J. Immunol.* 182:3510–3521. http://dx.doi.org/10.4049/jimmunol.0800854

Noman, M.Z., S. Buart, P. Romero, S. Ketari, B. Janji, B. Mari, F. Mami-Chouaib, and S. Chouaib. 2012. Hypoxia-inducible miR-210 regulates the susceptibility of tumor cells to lysis by cytotoxic T cells. *Cancer Res.* 72:4629–4641. http://dx.doi.org/10.1158/0008-5472.CAN-12-1383

Okazaki, T., and T. Honjo. 2007. PD-1 and PD-1 ligands: from discovery to clinical application. *Int. Immunol.* 19:813–824. http://dx.doi.org/10.1093/intimm/dxm057

Pardoll, D.M. 2012. The blockade of immune checkpoints in cancer immunotherapy. *Nat. Rev. Cancer.* 12:252–264. http://dx.doi.org/10.1038/nrc3239

Semenza, G.L. 2011. Oxygen sensing, homeostasis, and disease. *N. Engl. J. Med.* 365:537–547. http://dx.doi.org/10.1056/NEJMra1011165

Topalian, S.L., F.S. Hodi, J.R. Brahmer, S.N. Gettinger, D.C. Smith, D.F. McDermott, J.D. Powderly, R.D. Carvajal, J.A. Sosman, M.B. Atkins, et al. 2012. Safety, activity, and immune correlates of anti-PD-1 antibody in cancer. *N. Engl. J. Med.* 366:2443–2454. http://dx.doi.org/10.1056/NEJMoa1200690

West, E.E., H.T. Jin, A.U. Rasheed, P. Penaloza-Macmaster, S.J. Ha, W.G. Tan, B. Youngblood, G.J. Freeman, K.A. Smith, and R. Ahmed. 2013. PD-L1 blockade synergizes with IL-2 therapy in reinvigorating exhausted T cells. *J. Clin. Invest.* 123:2604–2615. http://dx.doi.org/10.1172/JCI67008

Youn, J.I., S. Nagaraj, M. Collazo, and D.I. Gabrilovich. 2008. Subsets of myeloid-derived suppressor cells in tumor-bearing mice. *J. Immunol.* 181:5791–5802.